BioNanoScience
https://doi.org/10.1007/s12668-022-01034-5

Evaluation of the Antimicrobial, Antioxidant, and Cytotoxicity Against MCF-7 Breast Cell Lines of Biosynthesized Vanadium Nanoparticles

Rasha Y. Abdel-Ghafar[1] · Amira E. Sehim[1] · Zeinab K. Hamza[2] · Aziza A. El-Nekeety[2] · Mosaad A. Abdel-Wahhab[2]

Accepted: 10 September 2022

Abstract

This study was carried out to synthesize and characterize vanadium nanoparticles (VNPs) using orange peel extract and to evaluate the antimicrobial, antioxidant, and anticancer activities of the biosynthesized VNPs. The antifungal activity was tested against *Fusarium graminearum*, *Alternaria alternata*, *Candida albicans*, *Aspergillus niger*, and *Aspergillus flavus*. However, the antibacterial activity was tested against Gram-positive bacteria (*Staphylococcus aureus* and *Bacillus cereus*) and Gram-negative bacteria (*Yersinia enterocolitica*, *Salmonella typhimurium*, and *Escherichia coli*). The antioxidant activity was determined using the DPPH assay, and the anticancer activity was tested against the MCF-7 breast cell line. The biosynthesized VNPs were mostly square with an average size of 80 ± 3 nm and zeta potential of − 50 ± 6 mV. VNPs showed strong antifungal and antibacterial activities at a concentration of 100 µg/mL against the tested fungi and bacteria. These biosynthesized VNPs showed strong antioxidant reaching 91.65% at a concentration of 2000 µg/mL. Moreover, the anticancer activity against MCF-7 breast cell line with IC50 reached 15.99 µg. Therefore, it could be concluded that VNPs with strong antimicrobial, antioxidant, and anticancer activities can be synthesized successfully using orange peel extract and can be used in pharmaceutical and medical applications.

Keywords Vanadium nanoparticles · Green synthesis · Antifungal · Antibacterial · Antioxidant · Anticancer

1 Introduction

Recently, vanadium oxide nanoparticles (VNPs) are widely used in different applications due to their physical and chemical characteristics. VNPs are used in different fields such as catalysts and sensors in the electrochemical, synthetic, and optical fields in addition to medical and biological applications [1–3]. VNPs can be synthesized by several methods including vacuum evaporation, hydrothermal, sol–gel, and ultrasonication routes [3, 4]. During the last decades, vanadium was used in medical purposes for the stimulation of metabolism and cellular growth, regeneration of bone, anti-diabetic effects, cardio- and neuro-protective properties, anticancer, anti-parasitic, anti-mutagenic, and antimicrobial [5–7].

In the biological media, vanadium releases some active components such as protonated vanadate under the biological conditions at pH 7.4 and in the presence of dissolved oxygen [8, 9]. The activities of vanadate were reported to be due to their similar structure to phosphate which leads to the reversible inhibition of the phosphate-dependent enzymes including protein tyrosine phosphatases [10, 11]. Additionally, the stabilization of peroxide vanadates as a strong oxidant leads to the irreversible inhibition of the cysteine groups in several active centers of the regulatory enzymes [5, 12]. The biological properties of vanadium nanoparticles depend on several factors including the derivative type, the dose, and the route of administration, the treatment period, and the sensitivity to the compound administrated [13]. Vanadium is associated with its oxidation degree (vanadate/vanadyl ion) and its chemical form (inorganic/organic ligand) [14, 15]. The presence of the different vanadate species is depending on the concentration of vanadium and the pH. Their occurrence can be explained by the protonation and the condensation

✉ Mosaad A. Abdel-Wahhab
mosaad_abdelwahhab@yahoo.com;
ma.abdelwahab@nrc.Sc.eg

[1] Botany and Microbiology Department, Faculty of Science, Benha University, Benha, Egypt

[2] Food Toxicology & Contaminants Department, National Research Centre, Cairo, Egypt

Published online: 22 September 2022

equilibrium. In the very dilute solutions, monomeric vanadium ions were found, and their concentration was increased, leading to polymerization, especially in the acidic solution [16, 17].

Plant-mediated synthesis of nanoparticles is valuable for biomedical applications due to their safety and cost-effectiveness [18]. Green synthesis concentrates on the removal or decreases the harmful substrates produced during the synthesis of NPs since it is safe and non-toxic used for the fabrication of biologically compatible NPs appropriate for several pharmaceutical and medical applications such as gene or drug delivery, protein labeling, pathogen detection, and tracking, and tissue engineering [19]. The most suitable living organisms used in the green synthesis of NPs are the plants, because of several reasons including their large-scale production, understanding of various biochemical compounds and pathways, low cost, and short production time as well as their non-toxic effect [20, 21]. The current study aimed to biosynthesize and characterize VNPs using orange peel extract and evaluate the antifungal, antibacterial, antioxidant, and anticancer activities of the biosynthesized VNPs.

2 Materials and Methods

2.1 Materials and Reagents

Orange peel waste after juice extraction was obtained from a local food processing company in Cairo. Vanadium (II) chloride (VCl_2), 1,1-diphenyl-2-picrylhydrazyl (DPPH), and ascorbic acid were purchased from Sigma Chemical Co. (St. Louis, MO, USA). Czapek-Dox's agar was obtained from DSMZ (GmbH, Germany). All chemicals and reagents used in this study were of analytical grade and purchased from Sigma-Aldrich (Taufkirchen, Germany).

2.2 Microorganisms

Fungal strains of *Alternaria alternata*, *Aspergillus niger*, *A. flavus*, and *Fusarium graminearum* were isolated from soil and cereal samples, and *Candida albicans* strain was provided by Microbiology Lab., Faculty of Science, Benha University, Egypt. Bacterial pathogenic strain *Bacillus cereus* B-3711 was provided by the Northern Regional Research Laboratory, IL, USA (NRRL), and *Yersinia enterocolitica* was obtained from the Hungarian National Collection of Medical Bacteria. However, *Escherichia coli* 0157:H7, *Salmonella typhimurium*, and *Staphylococcus aureus* were isolated from and serologically identified by the Dairy Microbiology Lab., National Research Center Dokki, Cairo, Egypt.

2.3 Synthesis and Characterization of VNPs

To obtain the aqueous extract of orange peel (OP), the OP was rinsed with tap water and then dried in shadow until constant weight. Fifty grams of the dried OP was poured into a container containing 500 mL boiling water for 4 h and then filtered using Whatman filter paper. The filtrate was used for the synthesis of vanadium nanoparticles (VNPs) as described by Aliyu et al. [22].

Two hundred milliliters of the aqueous solution of VCl_2 (1 mM) was slowly added dropwise to10 mL of OP extract with constant stirring for 2 h on a magnetic stirrer for the reduction of V^{2+} into V^0 until the color was changed [23, 24]. The mixture was then centrifuged at room temperature for 20 min at 10,000 rpm. The supernatant was discarded; the pellet was re-dispersed in distilled water and lyophilized to dryness and stored at room temperature for future use [21]. Scanning electron micrographs (SEM) for VNPs were recorded on JEOL JAX-840A and JEOL JEM-1230 electron micro-analyzers, respectively. The particle was coated with a gold coating to have good conductivity [25]. Zeta potential and average diameter were calculated using a particle size analyzer (Nano-ZS, Malvern Instruments Ltd., UK). The FTIR spectrum of VNPs was carried out using an infrared spectrometer (FTIR) (Nicolet iS10, Thermo Fisher Scientific Inc., USA) to identify the possible biomolecules responsible for capping and efficient stabilization of VNPs synthesized using OP extract. VNP pellets were washed with 20 mL distilled water 3 times to get rid of all the free proteins/enzymes that were not capping the VNPs before the FTIR measurement.

2.4 Antifungal Activity of VNPs

The antifungal potential of VNPs was evaluated by the agar well diffusion technique as described by El Sayed et al. [26]. The spores of individual fungi were grown in Petri dishes containing Czapek-Dox's agar containing sucrose, $NaNO_3$, KH_2PO_4, $MgSO_4.7H_2O$, KCL, $FeSO_4.7H_2O$, and agar in concentrations of 30, 3, 1, 0.5, 0.01, and 20 g/L, respectively. The Petri dishes were inoculated with the spore suspension (10^7 spore/mL) of the tested fungal species. However, *C. Albicans* (10^7 cells/mL) was cultured in a Petri dish containing Sabouraud's glucose agar containing bactropeptone, KH_2PO_4, glucose, $MgSO_4.7H_2O$, and agar in concentrations of 10, 1, 20, 1, and 20, respectively. After inoculation, wells of standard diameter (8 mm) were bored in the medium using a sterile well puncher at an equal distance. VNP solution was added into open wells at different concentrations (25, 50, and 100 µg/mL). Negative controls were made using wells

congaing DMSO only and fluconazole at a concentration of 50 µg/mL was used as the positive control. Plates were incubated at 30 °C for 5 days and then examined at the end of the incubation period and the diameter of the zone of inhibition (ZOI) was recorded as mean values ($n = 3$) and was expressed in millimeter (mm).

2.5 Antibacterial Activity of VNPs

The diameters of inhibition zones were estimated by the disk diffusion method as described by Tamokou et al. [27], with some modifications. The solution of VNPs was prepared at a concentration of 1 mg/mL for antibacterial assay, and the sterile disks were impregnated with 10 µL of each for antibacterial assay (10 µg/disk) for each inoculated spread plate. The disks of samples were placed on the surface of the agar plate using sterile forceps and gently press down each disk to ensure complete contact with the agar surface. The assessment of antimicrobial activity was conducted against Gram-positive bacteria (*Staphylococcus aureus* and *Bacillus cereus*) and Gram-negative bacteria (*Yersinia enterocolitica*, *Salmonella Typhimurium*, and *Escherichia coli*). Cefoperazone was used as a positive control for bacteria at a concentration of 100 µg/mL, while DMSO solution (10% v/v) was used as a negative control. The plates were incubated at 37 °C for 18 h. The diameter of zones of complete inhibition was measured to the nearest whole millimeter, including the diameter of the disk using sliding calipers that were held on the back of the inverted Petri plate. Plates were examined for growth inhibition and the diameter of the inhibition zone was measured. The strength of the activity was classified as high activity for the inhibition zone having diameters of 10–15 mm, low activity for the diameter ranging from 7 to 10 mm, and no activity for one with a diameter less than 7 mm.

2.6 Antioxidant Activity of VNPs

The in vitro antioxidant activity of VNPs was assessed by 2.2-diphenyl-1-picrylhydrazyl (DPPH) free radical scavenging assay according to the method of Brand-Williams et al. [28] with slight modification. The stock solution was prepared by dissolving 24 mg DPPH in 100 mL methanol (80%) and then stored at 20 °C until needed. The working solution was adjusted to an absorbance of about 0.750 ± 0.02 at 517 nm using the spectrophotometer. An aliquot of 1 mL DPPH solution was mixed with 100 µL of VNPs at varying concentrations (2000, 1000, 500, 250,125, 62.5 µg/mL). The reaction mixture was mixed vigorously and left in the dark at room temperature for 30 min. The transformation between the oxidized (initial, violet) and reduced (end-product, yellow) form of DPPH was followed by recording the absorbance decrease at 517 nm against a blank, i.e., without DPPH with a UV–Vis Shimadzu (UV-1601, PC) spectrophotometer using 10 mm polystyrene. Methanol was used for zero spectrophotometer, and the measurement was performed in triplicate and an average was used. The radical scavenging activity was expressed as percentage inhibition of DPPH using the following formula:

$$\%\text{Inhibition} = \left[\left(A_{\text{control}} - A_{\text{treatment}}/A_{\text{control}}\right)\right] \times 100$$

where A_{control} is the absorbance of the control and $A_{\text{treatment}}$ is the absorbance of the treatments. Ascorbic acid was used as a reference compound. Then, % of inhibition was plotted against concentration, and the IC_{50} value was calculated by graphical method.

2.7 Cytotoxicity of VNPs

Cell line: Mammary gland (MCF-7) cell lines were obtained from ATCC via Holding company for biological products and vaccines (VACSERA), Cairo, Egypt.

MTT assay: This assay was carried out according to the method described by Mosmann and Immunol [29]. In this assay, the VNPs were used to determine the inhibitory effects on cell growth. This colorimetric assay is based on the conversion of the yellow tetrazolium bromide (MTT) to a purple formazan derivative by mitochondrial succinate dehydrogenase in viable MCF-7 cell lines. Cell lines were cultured in RPMI-1640 medium (Sigma Co. St. Louis, USA) with 10% fetal bovine serum (GIBCO, UK). Antibiotics (100 units/mL penicillin and 100 µg/mL streptomycin) were added to the media and incubated at 37 °C in a 5% Co_2 incubator. Then, the cell lines were seeded in a 96-well plate at a density of 1.0×10^4 cells/well at 37 °C for 48 h and under 5% Co_2. After the incubation period, the cells were treated with different concentrations of VNPs and incubated for 24 h. After 24 h of the treatment, 20 µL of MTT (Sigma, St., USA) solution at 5 mg/mL was added and incubated for 4 h. Dimethyl sulfoxide (DMSO; Sigma, St., USA) in a volume of 100 µL was added into each well to dissolve the purple formazan formed. The colorimetric assay was measured and recorded at the absorbance of 570 nm using a plate reader (EXL 800, USA). The relative cell viability in percentage was calculated as follows:

(A570 of treated samples/A570 of the untreated sample) × 100.

2.8 Statistical Analysis

The data were gathered and given into the "SPSS-24" computer software program and was analyzed by "one-way

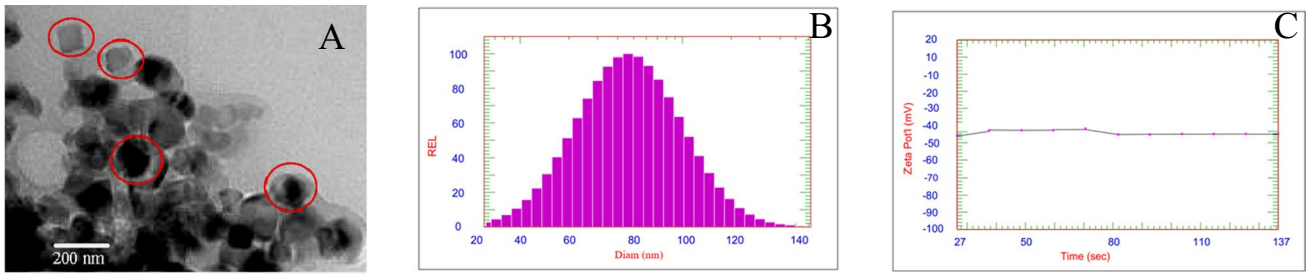

Fig. 1 **A** TEM image of VNPs showing particle shape and size. **B** DLS analysis showing the size distribution of VNPs. **C** Zetasizer chromatogram showing the zeta potential of VNPs

ANOVA" and then the Duncan post hoc test ($p < 0.01$). The results were expressed as mean ± SD.

3 Results and Discussion

3.1 Characterization of VNPs

The current results showed that VNPs were successfully biosynthesized using OP extract by the addition of VCl_2 (1 mM) dropwise to 10 mL of OP extract with constant stirring for 2 h at room temperature. The TEM image of the synthesized VNPs showed that the particles are mostly square (Fig. 1A). The dynamic light scattering (DLS) showed that the average particle size of VNPs was 80 ± 3 nm (Fig. 1B) and the zeta potential was − 50 ± 6 mV (Fig. 1C). This is probably because of the availability of various amounts of the capping agents in the extract which was confirmed by the differences in the peak regions obtained by the FTIR results. The square shape of the biosynthesized VNPs is different from that developed in previous studies which reported spherical shape VNPs [1, 3]. This difference may be due to the different extracts used in the biosynthesis of VNPs and/or the vanadium salt used [30]. On the other hand, the negative zeta potential reported herein may be due to the capping of several natural constituents in OP extract [31]. The negative zeta potential suggested the strong repellent force between the particles because of the higher electrical charge on the surface of VNPs that showed higher stability and prevent the aggregation between the particles [32].

The FTIR spectra of OP extract showed distinct peaks in the range of 3334.75 and 550.33 cm^{-1} (Fig. 2). The peaks at 3334.75–4089.82 cm^{-1} are referring to the stretching vibration of the O–H group [30]. However, the peaks at 1744.63–1534.33 cm^{-1} are due to the amide which is characteristic of protein and mostly indicated the predominantly surface capping of the space with the C = O group which is responsible for the stabilization [31]. Additionally, the frequency of OH absorption and the intense absorption was noticed at 1744.63 cm^{-1} which is characteristic of the C = C stretching aromatic ring. However, the peak at 2981.67 cm^{-1} indicated the specific absorption of the carbonyl group. The peak at 1025.75 cm^{-1} may be assigned to the C-H stretching of the aromatic carbonyl group. Therefore, these observations suggested the occurrence of some terpenoids, phenolic compound (OH) proteins, and flavones that are bounded to the surface of VNPs. On the other hand, the changes in FTIR spectra of the biosynthesized VNPs after the bioreduction suggested that the participation of proteins and tarperoidpolyols has amides, carboxylic acid, and alcohols as functional groups responsible for the bioreduction. However, the terpenoids may not be involved in the reduction of VCl_3 due to their being poorly water-soluble [22]; meanwhile, proteins probably showed little importance in the biosynthesis of NPs [33]. Hence, the water-soluble flavonoid compounds and phenolic acid are suggested to have a major role in the reaction involved in the bioreduction of the synthesized NPs [34].

3.2 Antifungal Activity

The results presented in Table 1 showed moderate antifungal activity against the tested pathogenic fungi at the low dose

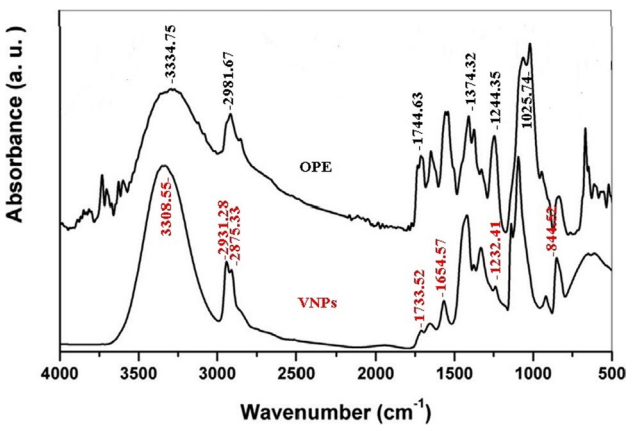

Fig. 2 FTIR spectra of VNPs and orange peel extract (OPE)

Table 1 Antifungal activity of biosynthesized VNPs against different pathogenic fungi

Pathogenic fungal isolates	Fluconazole	VNPs		
	50 µg/mL	25 µg/mL	50 µg/mL	100 µg/mL
F. graminearum	22.4 ± 0.14	5.3 ± 0.11	22.7 ± 0.21	39.6 ± 0.15
A. alternata	18.2 ± 0.24	8.4 ± 0.12	20.6 ± 0.24	24.3 ± 0.05
C. albicans	23.3 ± 0.31	5.7 ± 0.11	23.4 ± 0.23	30.5 ± 0.11
A. niger	18.5 ± 0.13	6.4 ± 0.13	18.3 ± 0.17	24.3 ± 0.11
A. flavus	16.7 ± 0.12	3.7 ± 0.11	14.3 ± 0.16	18.4 ± 0.12

ZOI was measured in mm and expressed as mean ± SD for 3 replicates

(25 µg/mL). At a concentration of 50 µg/mL, VNPs showed antifungal activity similar to fluconazole. However, at 100 µg/mL, VNPs were more effective than fluconazole and the maximum ZOI recorded was 24.3, 30.5, 24.3, and 18.4 mm for *F. graminearum*, *A. alternate*, *C. albicans*, *A. niger*, and *A. flavus*, respectively. The results also showed that *F. graminearum* was the most affected by ZOI at the higher concentration (100 µg/mL) and the less affected was *A. flavus.* These results were similar to the results of Gholami-Shabani et al. [31] who reported that VNPs biosynthesized using cell-free filtrate of *Fusarium oxysporum* showed strong antifungal activity against *F. graminearum*, *A. fumigatus*, *A. niger*, *A. flavus*, *A. alternata*, and *P. citrinum*. The fungicidal activity of different metal nanoparticles depends on the shape and the size of the particles. Wani and Ahmad [35] observed that small-sized nanodisks induced intracellular acidification and death of a cell due to the inhibition of H + ATPase. Moreover, NPs induce deformation in the hyphae of fungi and inhibit the transition of hyphal which probably lead to fungicidal activity [36, 37].

3.3 Antibacterial Activity

The results of antibacterial activity of VNPs against Gram-positive (*S. aureus* and *B. subtilis*) and Gram-negative (*E. coli*, *S. typhimurium*, and *Y. enterocolitica*) bacteria using the diffusion technique compared with cefoperazone as a reference antibacterial agent are summarized in Table 2. The results showed that VNPs exhibited antibacterial activities that varied among the tested microbial strains. At the low dose of 25 µg/mL, VNPs showed a weak antibacterial activity, and this activity increased by increasing the dose of VNPs and reached its maximum at 100 µg/mL. Moreover, the concentration of 100 µg/mL VNPs induced a diameter inhibition zone of 15.4 and 25.3 nm for *S. aureus* and *B. subtilis*, respectively; however, it induced DIZ of 24.4, 26.1, and 21.9 nm for *E. coli*, *S. typhimurium*, and *Y. enterocolitica*, respectively. It was reported that metal nanoparticles showed antibacterial activity against Gram-positive and Gram-negative bacteria based on their concentration, capping method, and size [38]. The composition of the cell wall of Gram-negative strains consists of a thin layer (~ 7–8 nm) of peptidoglycan polymer, and their surfaces carry negative charges [39]. These features are linked directly to the antibacterial properties of NPs, as these NPs can easily penetrate the thin cell wall of bacteria. In addition, the negative surface charge encourages the electrostatic interaction between NPs and the cells resulting in oxidative stress due to the production of ROS (reactive oxygen species) as shown by Sharmin et al. [40]. This action leads to the destruction and inhibition of the bacterial cell [41, 42]. On the other hand, Gram-positive bacteria showed better permeability toward different substances because they only contain the outer peptidoglycan layer and not the polysaccharide membrane, which contains structural lipopolysaccharides [43]. Moreover, the smaller negative charges on their surface promote the penetration of NPs and allow the entrance of the negatively charged peroxide ions and superoxide radicals to ensure the destruction of the cell at a relatively low level [44, 45]. Additionally, the generation of oxidative stress and the excess of ROS production due to NPs induce the bacterial protein and DNA damage of some Gram-positive and negative strains [46].

Table 2 Antibacterial activity of biosynthesized VNPs against Gram-positive and Gram-negative bacteria (results are expressed as inhibition zone diameter in mm)*

Concentrations	Gram-positive		Gram-negative		
	S. aureus	*B. cereus*	*E. coli*	*S. typhimurium*	*Y. enterocolitica*
25 µg/mL	5.7 ± 0.21	8.2 ± 0.57	7.6 ± 0.65	6.8 ± 0.41	8.9 ± 0.74
50 µg/mL	9.2 ± 0.17	14.5 ± 1.10	12.3 ± 0.47	11.4 ± 0.23	15.5 ± 0.27
100 µg/mL	15.4 ± 0.22	25.3 ± 1.12	24.3 ± 0.61	26.1 ± 0.17	21.9 ± 0.82
Cefoperazone	**	**	**	**	**

*The zone of inhibition values was expressed as mean ± SD

**DIZ was too big to be measured

3.4 Antioxidant Activity

It is well known that orange peel is rich in vitamin C and other flavonoids which possess potent antioxidant activity. Luteolin is a bioflavonoid and is well known for its good antioxidant and radical scavenging activity and to form a chelate with transition metals. The formation of metal and flavonoid complex cations changes its natural free radical scavenging ability, signifying that the complex has increased ability to scavenge oxidants and free radicals. DPPH test shows that the antioxidants have the potential to reduce the DPPH radical from violet to yellow-colored diphenyl-picrylhydrazine. In the chemical reaction, antioxidants donate the hydrogen to DPPH and convert it into DPPH-H. Hence, the DPPH method was used to evaluate the antioxidant activity of both compounds. The antioxidant activity of flavonoids and vanadium complexes is depending on their structure and their ability to donate hydrogen. The reaction between DPPH and flavonoids occurs through two main steps including the very quick diminishes of DPPH absorbance and in the second step, the absorbance of DPPH diminishes slowly within about 1 h to reach the constant or fixed value. The last step is corresponding to the abstraction of the most responsible H-atom, while the slow step displays the oxidative degradation in the remaining product. Although the antioxidant activity of any compound depends on the molecular structures of the compound, the complexation made with the metal ions probably affects the chemical characteristics of the flavonoid molecules, and hence, the activity is varied [47]. The current results are in an agreement with those reported previously and suggest that the coordination complex affected the parent antioxidant ability. In the current study, we evaluated the antioxidant activities of different concentrations of VNPs. The antioxidant activity of the biosynthesized VNPs reached 91.65% at a concentration of 2000 µg/mL, while it was 98.73% for ascorbic acid at the same concentration (Table 3) with IC50 of 292.2 and 47.68 µg/mL for VNPs and ascorbic acid, respectively (Fig. 3). This antioxidant activity was reduced by decreasing the concentration to reach 46.27% and 80.28% for VNPs and ascorbic acid, respectively. However, the lower concentration of VNPs did not show any antioxidant activity. These results suggested that flavonoids and vitamin C in the VNPs scavenged the free radicals at the high concentration, and thus, it represented a potent inhibitory effect. Moreover, the antioxidant activity of the biosynthesized VNPs may be due to the coordination of the metal in position numbers 4 and 5 of its condensed ring system increasing its ability to stabilize the unpaired electrons, leading to the free radical scavenging activity [30, 48].

Table 3 DPPH radical scavenging activity of VNPs and standard ascorbic acid as a reference

Conc. µg/mL	Ascorbic acid	Vanadium NPs
2000	98.73 ± 0.033	91.63 ± 0.067
1000	98.55 ± 0.084	88.23 ± 0.11
500	98.24 ± 0.13	85.53 ± 0.17
250	80.28 ± 0.36	46.267 ± 7.78
125	62.69 ± 0.60	–
62.5	51.26 ± 2.56	–
31.25	41.82 ± 1.03	–

Values are expressed as mean ($n = 3$) ± SD of the percent inhibition of the absorbance of DPPH radicals

3.5 Anticancer Activity

The results of anticancer activity of VNPs against MCF-7 breast cell lines exposed to different concentrations of VNPs using MTT assay indicated that the viability of MCF-7 cell lines was increased by the decrease of VNP concentration (Fig. 4) and the calculated IC_{50} of VNPs was 15.99 µg which indicated a strong anticancer activity (Fig. 5). Similar results were reported by Gholami-Shabani et al. [31]. A previous report showed that the anticancer activity of natural products is mainly due to their antioxidant activity [49]. Hence, the anticancer activity of biosynthesized VNPs seems to be related to the antioxidant activity of different compounds in orange peel extract such as the flavonoids, vitamin C, alkaloids, tannins, and saponins [50, 51]. In the current study, the antioxidant activity assay using DPPH showed that the IC_{50} of VNPs was 292.2 µg/mL, supporting our hypothesis that the antioxidant property is one of the suggested mechanisms of the anticancer activity of VNPs against MCF-7 breast cell lines. Moreover, the size, shape, and texture of metallic NPs play an important role in their therapeutic activities. The small size of metallic NPs allows them to penetrate the cell membrane and enter the cell to exert their anticancer activity against different cell lines [52, 53]. In this concern, several studies reported

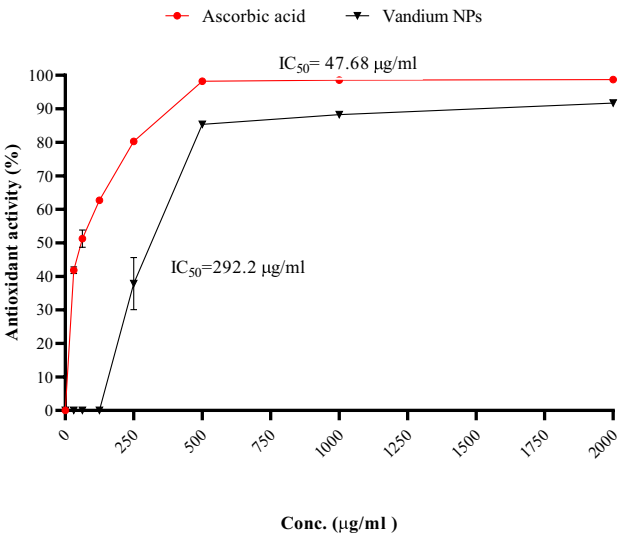

Fig. 3 DPPH radical scavenging activity of VPs and standard ascorbic acid as a reference. Values are expressed as mean ($n = 3$) of the percent inhibition of the absorbance of DPPH radicals

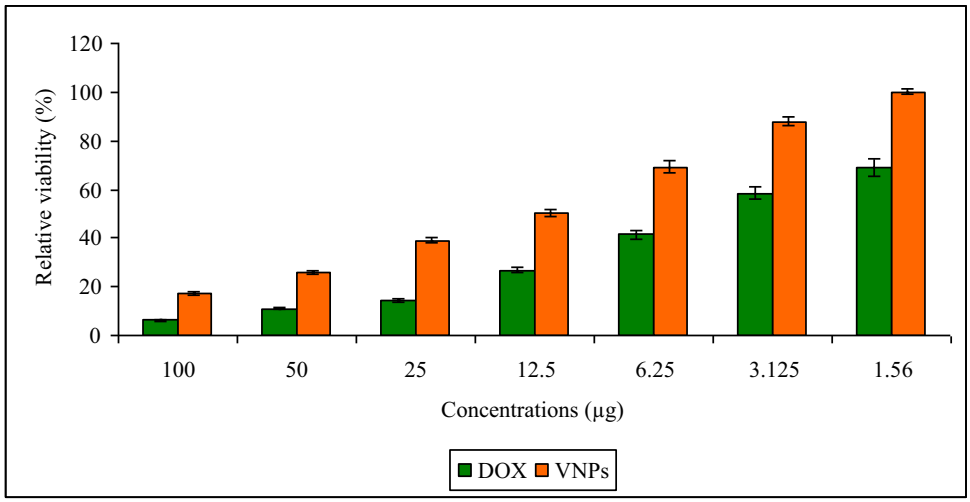

Fig. 4 Average of relative viability (%) of VNPs against MCF-7 cells. The data presented as mean ± SD for three replicates

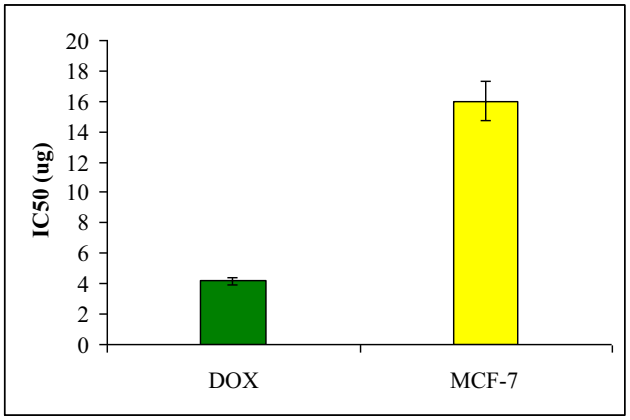

Fig. 5 The IC_{50} of VNPs in MCF-7 breast cell lines. The data presented as mean ± SD for three replicates

the anticancer activity of metallic NPs against different cell lines [50, 54]. VNPs also were reported to have a strong anticancer activity against malignant cervical cell lines and MCF-7 breast cell lines [30, 31]; in addition, the biosynthesized VNPs reduce the tumor volume via the free radical scavenging properties [55] which cause countless chain reactions resulting in the generation of more free radical leading to different mutations in DNA and RNA structure and the uncontrolled increase in the proliferation of malignant cells [56, 57]. Therefore, angiogenesis and tumorigenesis are developed due to the high levels of free radicals in all kinds of cancer [55–57]. The current results supported the earlier studies which indicated that the biosynthesized VNPs have a vital role in the elimination of free radicals and consequently prevent the growth of different malignant cells [31, 58].

4 Conclusion

The results of the current study revealed that VNPs with a particle size of 80 ± 3 nm and zeta potential of − 50 ± 6 mV were successfully synthesized using orange peel extract. The biosynthesized VNPs showed strong antifungal activity against *F. graminearum*, *A. alternate*, *C. albicans*, *A. niger*, and *A. flavus*. These particles also showed strong antibacterial activity against Gram-positive and Gram-negative bacteria. The effective concentration for the antimicrobial activity of VNPs was at a concentration of 100 µg/mL. The biosynthesized VNPs also showed strong antioxidant and DPPH radical scavenging activity at a concentration of 2000 µg/mL with a recorded IC_{50} of 292.2 µg/mL. VNPs also showed anticancer efficiency against the MCF-7 breast cell line at a concentration of 100 µg. Therefore, green synthesis seems a promising approach for the development of VNPs with strong antimicrobial, antioxidant, and anticancer activities and could be used widely in pharmaceutical and medical applications.

Author Contribution This work was carried out in collaboration between all authors. Authors RY Abdel-Ghafar, AE Sehim, ZK Hamza, and AA El-Nekkety carried out the experimental work, managed the literature searches, and shared in writing the first draft of the manuscript. Author MA Abdel-Wahhab wrote the protocol, managed the project, managed the analyses of the study, performed the statistical analysis, and wrote the final draft of the manuscript. All authors read and approved the final manuscript.

Funding This work was supported by the National Research Centre, Dokki, Cairo, Egypt, project # 12050305.

Data Availability NA.

Declarations

Ethics Approval NA.

Informed Consent NA.

Consent for Publication NA.

Conflict of Interest The authors declare no competing interests.

References

1. Aliyu, A., Garba, S., & Bognet, O. (2017). Green synthesis, characterization and antimicrobial activity of vanadium nanoparticles using leaf extract of Moringa Oleifera. *International Journal Chemical Sciences, 16*, 231. Corpus ID: 201647732.
2. Deepika, P., Vinusha, H., Muneera, B., Rekha, N., & Prasad, K. S. (2020). Vanadium oxide nanorods as DNA cleaving and anti-angiogenic agent: Novel green synthetic approach using leaf extract of *Tinosporacordifolia*. *Current Research in Green Sustainable, 1–2*, 14–19.
3. Karthik, K., Nikolova, M. P., Phuruangrat, A., Pushpa, S., Revathi, V., & Subbulakshmi, M. (2020). Ultrasound-assisted synthesis of V2O5 nanoparticles for photocatalytic and antibacterial studies. *Materials Research Innovations, 24*, 229–234.
4. Talavera, N., Navarro, M., Sifontes, A., Díaz, Y., Villalobos, H., Nino-Vega, G., Boada-Sucre, A., & Gonzalez, I. (2013). Green synthesis of nanosized vanadium pentoxide using *Saccharomyces cerevisiae* as biotemplate. *Recent Research Developments in Materials Science, 10*, 89–102.
5. Pessoa, J. C., Etcheverry, S., & Gambino, D. (2015). Vanadium compounds in medicine. *Coordination Chemistry Reviews, 301*, 24–48.
6. Rehder, D. (2016). Perspectives for vanadium in health issues. *Future Medicinal Chemistry, 8*(3), 325–338. https://doi.org/10.4155/fmc.15.187
7. Crans, D. C., Yang, L., & Haase, A. (2018). Yang X (2018) Health benefits of vanadium and its potential as an anticancer agent. *Metal Ions in Life Sciences, 18*, 251–280.
8. Crans, D. C., Koehn, J. T., Petry, S. M., Glover, C. M., Wijetunga, A., Kaur, R., Levina, A., & Lay, P. A. (2019). Hydrophobicity may enhance membrane affinity and anti-cancer effects of Schiff base vanadium(V) catecholate complexes. *Dalton Transactions, 48*, 6383–6395.
9. Costa, B. C., Tokuhara, C. K., Rocha, L. A., Oliveira, R. C., Lisboa-Filho, P. N., & Costa Pessoa, J. (2019). Vanadium ionic species from degradation of Ti-6Al-4V metallic implants: In vitro cytotoxicity and speciation evaluation. *Materials Science & Engineering C Materials for Biological Applications, 96*, 730–739.
10. Irving, E., & Stoker, A. W. (2017). Vanadium compounds as PTP inhibitors. *Molecules, 22*, E2269.
11. McLauchlan, C. C., Kissel, D. S., & Herlinger, A. W. (2015). 2,2′-[N, N'-Bis (pyridin-2-ylmethyl) cyclohexane-trans-1,2-diyldi (nitrilo)] diacetato} cobalt (III) hexafluoridophosphate. *Acta Crystallographica Section E, 71*, 380–384.
12. Kioseoglou, E., Petanidis, S., Gabriel, C., & Salifoglou, A. (2015). The chemistry and biology of vanadium compounds in cancer therapeutics Coord. *Chemical Reviews, 301–302*, 87–105.
13. Gill, P., Moghadam, T. T., & Ranjbar, B. (2010). Differential scanning calorimetry techniques: Applications in biology and nanoscience. *Journal of Biomolecular Techniques, 21*(4), 167–193.
14. Nagesh, G. Y., Raj, K. M., & Mruthyunjayaswamy, B. H. M. (2015). Synthesis, characterization, thermal study and biological evaluation of Cu(II), Co(II), Ni(II) and Zn(II) complexes of Schiff base ligand containing thiazole moiety. *Journal of Molecular Structure, 1079*, 423–432.
15. Nagesh, G. Y., & Mruthyunjayaswamy, B. H. M. (2015). Synthesis, characterization and biological relevance of some metal (II) complexes with oxygen, nitrogen and oxygen (ONO) donor Schiff base ligand derived from thiazole and 2-hydroxy-1-naphthaldehyde. *Journal of Molecular Structure, 1085*, 198–206.
16. Domingo, J. L. (2002). Vanadium and tungsten derivatives as antidiabetic agents: A review of their toxic effects. *Biological Trace Element Research, 88*(2), 97–112.
17. Evangelou, A. M. (2002). Vanadium in cancer treatment. *Critical Reviews Oncology Hematologoy, 42*(3), 249–265.
18. Mobaraki, F., Momeni, M., Jahromi, M., Kasmaie, F. M., Barghbani, M., Taghavizadeh Yazdi, M. E., Meshkat, Z., Shandiz, F. H., & Hosseini, S. M. (2022). Apoptotic, antioxidant and cytotoxic properties of synthesized AgNPs using green tea against human testicular embryonic cancer stem cells. *Process Biochemistry, 119*, 106–118.
19. Shakerimanesh, K., Bayat, F., Shahrokhi, A., Baradaran, A., Yousefi, E., Mashreghi, M., Es-Haghi, A., Taghavizadeh Yazdi, ME. (2022). Biomimetic synthesis and characterisation of homogenouse gold nanoparticles and estimation of its cytotoxity against breast cancer cell line. *Materials Technology*. https://doi.org/10.1080/10667857.2022.2081287
20. Mousavi-Kouhi, S. M., Beyk-Khormizi, A., Mohammadzadeh, V., Ashna, M., Es-haghi, A., Mashreghi, M., Hashemzadeh, V., Mozafarri, H., Nadaf, M., & Taghavizadeh Yazdi, M. E. (2022). Biological synthesis and characterization of gold nanoparticles using Verbascum speciosum Schrad. and cytotoxicity properties toward HepG2 cancer cell line. *Research on Chemical Intermediates, 48*, 167–178. https://doi.org/10.1007/s11164-021-04600-w
21. Taghavizadeh Yazdi, M. E., Darroudi, M., Amiri, M. S., Zarrinfar, H., Hosseini, H. A., Mashreghi, M., Mozafarri, H., Ghorbani, A., & Mousavi, S. H. (2022). Antimycobacterial, anticancer, antioxidant and photocatalytic activity of biosynthesized silver nanoparticles using Berberis integerrima. *Iranian Journal of Science and Technology Transactions Science, 46*, 1–11. https://doi.org/10.1007/s40995-021-01226-w
22. Aliyu, A. O., Garba, S., & Bognet, O. (2018). Green synthesis, characterization and antimicrobial activity of vanadium nanoparticles using leaf extract of *Moringa oleifera*. *IOSR-JAC, 11*(1), 42–48.
23. Jain, D., Daima, H. K., Kachhwaha, S., & Kothari, S. L. (2009). Synthesis of plant-mediated silver nanoparticles using papaya fruit extract and evaluation of antimicrobial activities. *Digest Journal of Nanomaterials and Biostructures, 4*, 557–563.
24. Song, J. Y., Jang, H. K., & Kim, B. S. (2009). Biological synthesis of gold nanoparticles using *Magnolia kobus* and *Diopyros kaki* leaf extracts. *Process Biochemistry, 2009*, 1133–1138. https://doi.org/10.1016/j.procbio.2009.06.0
25. Ghosh, N., Paul, S., Basak, P. (2014). Silver nanoparticles of *Moringa oleifera*- green synthesis, characterisation and its antimicrobial efficacy. *Journal of Drug Delivery and Therapeutics*, 42–46. https://doi.org/10.22270/JDDT.V0I0.906
26. El-Sayed, E. S. R., Abdelhakim, H. K., & Zakaria, Z. (2020). Extracellular biosynthesis of cobalt ferrite nanoparticles by *Monascus purpureus* and their antioxidant, anticancer and antimicrobial activities: Yield enhancement by gamma irradiation. *Materials Science and Engineering C, 107*, 110318. https://doi.org/10.1016/j.msec.2019.110318
27. Tamokou, J. D., Tala, F. M., Wabo, K. H., Kuiate, J. R., & Tane, P. (2009). Antimicrobial activities of methanol extract and compounds from stem bark of *Vismia rubescens*. *Journal of Ethnopharmacology, 124*, 571–575.
28. Brand-Williams, W., Cuvelier, M. E., & Berset, C. (1995). Use of a free radical method to evaluate antioxidant activity. *Lebenson Wiss Technology, 28*, 25–30.

29. Mosmann, T. (1983). Rapid colorimetric assay for cellular growth and survival: Application to proliferation and cytotoxicity assays. *Journal of Immunological Methods, 65*, 55–63.
30. Zhang, Y., Zhang, X., Zhang, L., Alarfaj, A., Hirad, A., & Alsabri, A. (2021). Green formulation, chemical characterization, and antioxidant, cytotoxicity, and anti-human cervical cancer effects of vanadium nanoparticles: A pre-clinical study. *Arabian Journal of Chemistry, 14*, 103147. https://doi.org/10.1016/j.arabjc.2021.103147
31. Gholami-Shabani, M., Sotoodehnejadnematalahi, F., Shams-Ghahfarokhi, M., Eslamifar, A., Razzaghi-Abyaneh, M. (2021). Mycosynthesis and physicochemical characterization of vanadium oxide nanoparticles using the cell-free filtrate of *Fusarium oxysporum* and evaluation of their cytotoxic and antifungal activities. *Journal of Nanomaterials*, 2021 Article ID 7532660:12. https://doi.org/10.1155/2021/7532660
32. Taylor, P., Kusper, M., Hesabizadeh, T., Geoffrion, L. D., Watanabe, F., Herth, E., & Guisbiers, G. (2021). Synthesis of naked vanadium pentoxide nanoparticles. *Nanoscale Advance, 3*, 954–1961.
33. Huang, J., Li, Q., Sun, D., Lu, Y., Su, Y., Wang, Y. H., Wang, Y., Shao, W., & He, N. (2007). Biosynthesis of silver and gold nanoparticles by novel sundried *Cinnamomum camphora* leaf. *Nanotechnol, 18*(10), 105104J. https://doi.org/10.1088/0957-4484/18/10/105104
34. Elumalai, K., Velmurugan, S., Ravi, S., Kathiravan, V., & Ashokkumar, S. (2015). Green synthesis of zinc oxide nanoparticles using *Moringa oleifera* leaf extract and evaluation of its antimicrobial activity. *Spectrochim Acta A Mol Biomol Spectrosc, 143*, 158–164. https://doi.org/10.1016/j.saa.2015.02.011
35. Wani, I. A., & Ahmad, T. (2012). Size and shape dependant antifungal activity of gold nanoparticles: A case study of Candida. *Colloids and Surfaces B Biointerfaces, 101*, 162–170.
36. Cousins, B. G., Allison, H. E., Doherty, P. J., Edward, C., Garvery, M. J., Martin, D. S., & Wiliams, R. L. (2007). Effect of a nanoparticulate silica substrate on cell attachment of Candida albicans. The Society for Applied Microbiology. *Journal of Applied Microbiology, 102*, 757–765.
37. He, L., Liu, Y., Mustapha, A., & Lin, M. (2011). Antifungal activity of zinc oxide nanoparticles against Botrytis cinerea and *Penicillium expansum*. *Microbiological Research, 166*(3), 207–215.
38. Slavin, Y. N., Asnis, J., H€ afeli, U. O., & Bach, H. (2017). Metal nanoparticles: Understanding the mechanisms behind antibacterial activity. *Journal of Nanobiotechnology, 15*(1), 1–20.
39. Halder, S., Yadav, K. K., Sarkar, R., Mukherjee, S., Saha, P., Haldar, S., & Sen, T. (2015). Alteration of zeta potential and membrane permeability in bacteria: A study with cationic agents. *Springer Plus, 4*(1), 1–14.
40. Sharmin, S., Rahaman, M. M., Sarkar, C., Atolani, O., Islam, M. T., & Adeyemi, O. S. (2021). Nanoparticles as antimicrobial and antiviral agents: A literature-based perspective study. *Heliyon, 7*(3), e06456. https://doi.org/10.1016/j.heliyon.2021.e06456
41. Chen, Q., Li, J., Wu, Y., Shen, F., & Yao, M. (2013). Biological responses of Gram-positive and Gram-negative bacteria to nZVI (Fe 0), Fe 2þ and Fe 3þ. *RSC Advances, 3*(33), 13835–13842.
42. Mai-Prochnow, A., Clauson, M., Hong, J., & Murphy, A. B. (2016). Gram positive and Gram negative bacteria differ in their sensitivity to cold plasma. *Science and Reports, 6*, 38610.
43. Cabeen, M. T., & Jacobs-Wagner, C. (2005). Bacterial cell shape. *Nature Reviews Microbiology, 3*(8), 601–610.
44. Padmavathy, N., & Vijayaraghavan, R. (2011). Interaction of ZnO nanoparticles with microbes-a physio and biochemical assay. *Journal of Biomedical Nanotechnology, 7*(6), 813–822.
45. Reddy, K. M., Feris, K., Bell, J., Wingett, D. G., Hanley, C., & Punnoose, A. (2007). Selective toxicity of zinc oxide nanoparticles to prokaryotic and eukaryotic systems. *Applied Physics Letters, 90*(21), 213902.
46. Mahdy, S. A., Raheed, Q. J., & Kalaichelvan, P. T. (2012). Antimicrobial activity of zero-valent iron nanoparticles. *International Journal of Modern Engineering Research, 2*(1), 578–581.
47. Ensafi, A. A., Hajiana, R., & Ebrahimib, S. (2009). Study on the interaction between Morin-Bi (III) complex and DNA with the use of methylene blue dye as a fluorophor probe. *Journal of the Brazilian Chemical Society, 20*, 266–276.
48. Roy, S., Mallick, S., Chakraborty, T., Ghosh, N., Singh, A. K., Manna, S., & Majumdar, S. (2015). Synthesis, characterization and antioxidant activity of luteolin-vanadium (II) complex. *Food Chemistry, 173*, 1172–1178. https://doi.org/10.1016/j.foodchem.2014.10.141
49. Aman, S., Gupta, U. K., Singh, D., & Khan, T. (2018). Herbal treatment for the ovarian cancer. *SGVU Journal of Pharmaceutical Research Education, 3*, 325–329.
50. Jalalvand, A. R., Zhaleh, M., Goorani, S., Zangeneh, M. M., Seydi, N., Zangeneh, A., & Moradi, R. (2019). Chemical characterization and antioxidant, cytotoxic, antibacterial, and antifungal properties of ethanolic extract of Allium saralicum RM Fritsch leaves rich in linolenic acid, methyl ester. *Journal of Photochemistry and Photobiology B: Biology, 192*, 103–112.
51. Vinay, C. H., Goudanavar, P., & Acharya, A. (2018). Development and characterization of pomegranate and orange fruit peel extract based silver nanoparticles. *JMMIHS, 4*(1), 72–85.
52. Mao, B. H., Tsai, J. C., Chen, C. W., Yan, S. J., & Wang, Y. J. (2016). Mechanisms of silver nanoparticle-induced toxicity and important role of autophagy. *Nanotoxicol, 10*, 1021–1040.
53. Tahvilian, R., Zangeneh, M. M., Falahi, H., Sadrjavadi, K., Jalalvand, A. R., & Zangeneh, A. (2019). Green synthesis and chemical characterization of copper nanoparticles using Allium saralicum leaves and assessment of their cytotoxicity, antioxidant, antimicrobial, and cutaneous wound healing properties. *Applied Organometallic Chemistry, 33*, e5234.
54. Abdoli, M., Sadrjavadi, K., Arkan, E., Zangeneh, M. M., Moradi, S., Zangeneh, A., Shahlaei, M., & Khaledian, S. (2020). Polyvinyl alcohol/Gum tragacanth/graphene oxide composite nanofiber for antibiotic delivery. *Journal of Drug Delivery Science and Technology, 60*, 102044.
55. Katata-Seru, L., Moremedi, T., Aremu, O. S., & Bahadur, I. (2018). Green synthesis of iron nanoparticles using *Moringa oleifera* extracts and their applications: Removal of nitrate from water and antibacterial activity against *Escherichia coli*. *Journal of Molecular Liquids, 256*, 296–304.
56. Beheshtkhoo, N., Kouhbanani, M. A. J., Savardashtaki, A., Amani, A. M., & Taghizadeh, S. (2018). Green synthesis of iron oxide nanoparticles by aqueous leaf extract of *Daphne mezereum* as a novel dye removing material. *Applied Physics A, 124*, 363.
57. Sangami, S., & Manu, B. (2017). Synthesis of green iron nanoparticles using *Laterite* and their application as a Fenton-like catalyst for the degradation of herbicide ametryn in water. *Environmental Technology & Innovation, 8*, 150–163.
58. Radini, I. A., Hasan, N., Malik, M. A., & Khan, Z. (2018). Biosynthesis of iron nanoparticles using *Trigonella foenum-graecum* seed extract for photocatalytic methyl orange dye degradation and antibacterial applications. *Journal of Photochemistry and Photobiology B: Biology, 183*, 154–163.